Flow Reversal and Heat Transfer of Fully Developed Mixed Convection in Vertical Channels

Chin-Hsiang Cheng,* Hong-Sen Kou,* and Wen-Hsiung Huang†
Tatung Institute of Technology, Taiwan, Republic of China

The present analysis is concerned with flow reversal phenomena and heat transfer characteristics of the fully developed laminar combined free and forced convection in the heated vertical channels. Three fundamental combinations of thermal boundary conditions on the respective wall surface (namely isoflux-isoflux, isoflux-isothermal, and isothermal-isothermal) are considered separately so as to investigate extensively their distinct influence on the flow pattern. Results of the velocity distribution and temperature distribution as well as the Nusselt number in terms of bulk mean temperature are carried out. Based on the analytical solutions obtained, flow reversal adjacent to the relatively colder wall is found to exist within the channel as *Re/Gr* is below than a threshold value, which is related to the thermal boundary conditions. Parameter zones for the occurrence of reversed flow are presented. Comparisons and verification are made using the existing numerical solutions at locations far downstream of developing flow.

Nomenclature

b = channel width
Gr = Grashof number, Eqs. (4)
g = gravitational acceleration
k = thermal conductivity of fluid
Nu = Nusselt number, Eq. (6)
P = dimensionless fluid pressure, Eq. (3)
Pr = Prandtl number, Eq. (3)
p = fluid pressure
Q_1 = dimensionless heat flux on wall surface 1, Eq. (17b)
q = heat flux on wall surface
Re = Reynolds number, Eq. (5)
r_H = ratio of wall heat fluxes, $=q_2/q_1$
r_T = ratio of wall temperature differences, $=(T_2-T_0)/(T_1-T_0)$
T = fluid temperature
T_m = bulk mean temperature of flow
U = dimensionless fluid velocity in x direction, Eq. (3)
u = fluid velocity in x direction
u_0 = mean fluid velocity
X,Y = dimensionless coordinate system, Eq. (3)
x,y = rectangular coordinate system
α = thermal diffusivity of fluid
β = coefficient of volumetric expansion of fluid
θ = dimensionless fluid temperature, Eqs. (4)
θ_m = dimensionless bulk mean temperature, Eq. (14)
$\bar{\theta}_1$ = generalized fluid temperature in terms of wall temperature on surface 1, Eqs. (34)
$\bar{\theta}_2$ = generalized fluid temperature in terms of wall temperature on surface 2, Eqs. (28)
ν = kinematic viscosity of fluid
ρ = fluid density
σ = constant defined by Eq. (7)

(Q_1)-(Q_2) = isoflux-isoflux boundary combination
(Q_1)-(T_2) = isoflux-isothermal boundary combination
(T_1)-(T_2) = isothermal-isothermal boundary combination

Subscripts

0 = ambient reference quantity
1,2 = wall surface 1 and 2

Introduction

THE problems of combined free and forced convection in symmetrically or asymmetrically heated vertical passages have recently received considerable attention because of their practical applications in modern electronic equipment, nuclear reactors, solar systems, and heat exchangers. Exact solutions as well as experimental observations for the buoyancy-assisted effect on fully developed laminar flows in circular tubes were presented by Hanratty et al.[1] in 1958. Their experimental studies clearly revealed the existence of flow reversal in the fully developed region at a low Reynolds number. For the configuration of concentric circular annulus under isoflux wall conditions, Kim[2] and Maitra and Raju[3] obtained analytical solutions of the fully developed flows in which reversed flow could also be found. Additionally, for rectangular or other noncircular ducts, some mixed convection fully developed solutions were obtained by Iqbal and co-workers.[4-6] In Ref. 4, at a high Rayleigh number, the region of negative velocity is observed from the solutions. A more generalized formulation for the fully developed mixed convection flow is available in Ref. 7.

More recently, in addition to these geometries, increasing attention is being focused on the mixed convection problems in vertical parallel-plate channels. Aung and Worku[8,9] performed numerical computations for the developing flow under asymmetric isothermal and isoflux wall conditions. Habchi and Acharya[10] presented their solutions for the case of symmetric isothermal walls as well as one wall isothermal and the other insulated. Considering the fully developed behavior under isothermal heating conditions, Aung and Worku[11] provided the theoretical solutions and showed that when the heating is asymmetric, reversed flow occurs if the parameter Gr/Re exceeds a certain threshold value.

According to these previous experimental and theoretical

Received Dec. 20, 1988; revision received July 7, 1989.

*Associate Professor, Department of Mechanical Engineering.
†Professor, Department of Mechanical Engineering.

investigations, it is recognized that when wall heating is sufficiently intense, flow reversal can occur in a buoyancy-assisted flow within vertical passages. Such a flow would have a profound influence on the heat transfer and stability of the flowfield.

It is evident that, even for fully developed flow, this phenomenon of flow reversal has not yet been adequately discussed. Aside from the results for asymmetric isothermal channels provided by Aung and Worku,[11] no other information is available about the occurrence of reversed flow in the fully developed region under other thermal boundary conditions. Such information, however, is needed for the understanding of flow pattern or thermal characteristic and hence is worthy of additional investigation.

The present paper presents some analytical solutions of the fully developed mixed convection flow in a vertical channel under various fundamental thermal boundary conditions. Based on these theoretical solutions, the reversed flow zones (or say, the criteria of flow reversal) for different heating conditions on walls can be further obtained.

For mixed convection problems, flow motion is affected by buoyant force. The temperature and velocity fields are strongly coupled with each other so that the values of Nusselt number in the fully developed regions may become dependent on the thermal boundary conditions and deviate from those of pure forced convection flows.

Three fundamental combinations of thermal boundary conditions on the walls are considered. These combinations can cover almost all of the thermal boundary conditions studied by the previous investigators:

Case 1: isoflux-isoflux $\left(\textcircled{Q_1}\text{-}\textcircled{Q_2}\right)$

Case 2: isoflux-isothermal $\left(\textcircled{Q_1}\text{-}\textcircled{T_2}\right)$
a) $Q_1 \neq 0$
b) $Q_1 = 0$

Case 3: isothermal-isothermal $\left(\textcircled{T_1}\text{-}\textcircled{T_2}\right)$
a) $T_1 \neq T_2$
b) $T_1 = T_2$

Note that cases 2 and 3 are individually subdivided into two possible situations because they require different mathematical treatments in the evaluation of fully developed Nusselt numbers.

In regard to the buoyancy-resisted flow (i.e., upflow is cooled), fluid velocity near the cooled wall is retarded. Hence, heat transfer was found to decrease with the increasing of the Rayleigh number,[9] and more pumping power will be consumed due to the additional resisting buoyant force. Furthermore, resisting buoyancy gives rise to an unstable flowfield[1] to which a laminar model could not be applied. Therefore, because of the practical application and the validity of the theoretical model, the present study is concerned only with buoyancy-assisted flow situations shown in Fig. 1.

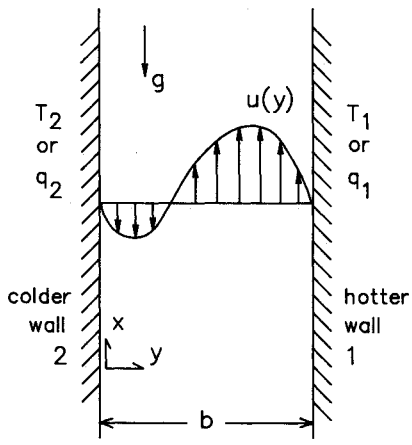

Fig. 1 Flow reversal of buoyancy-assisted flow in fully developed region of vertical channel.

Theoretical Analysis

The fluid properties are assumed constant, except for the variation of density in the buoyant term of the momentum equation, which is introduced by Boussinesq approximation. The dimensionless governing equations of momentum and energy conservations for the laminar, steady, fully developed, mixed convection flow are

$$0 = -\frac{dP(X)}{dX} + \frac{d^2U(Y)}{dY^2} + \theta(X,Y) \tag{1}$$

$$PrU(Y)\frac{\partial\theta(X,Y)}{\partial X} = \frac{\partial^2\theta(X,Y)}{\partial Y^2} \tag{2}$$

where the dimensionless quantities are

$$X = x/(bGr), \qquad Y = y/b, \qquad U = ub/(\nu Gr)$$

$$P = (p - p_0)b^2/(\rho\nu^2Gr^2), \qquad Pr = \nu/\alpha \tag{3}$$

and

$$\theta = k(T - T_0)/(q_1 b)$$
$$Gr = g\beta q_1 b^4/(\nu^2 k) \text{ for } \left(\textcircled{Q_1}\text{-}\textcircled{Q_2}\right) \tag{4a}$$

$$\theta = (T - T_0)/(T_2 - T_0)$$
$$Gr = g\beta(T_2 - T_0)b^3/\nu^2 \text{ for } \left(\textcircled{Q_1}\text{-}\textcircled{T_2}\right) \tag{4b}$$

$$\theta = (T - T_0)/(T_1 - T_0)$$
$$Gr = g\beta(T_1 - T_0)b^3/\nu^2 \text{ for } \left(\textcircled{T_1}\text{-}\textcircled{T_2}\right) \tag{4c}$$

The Reynolds number is defined by

$$Re = u_0 b/\nu \tag{5}$$

The Nusselt numbers in terms of bulk mean temperature T_m are given as

$$Nu_i = q_i b/[k(T_i - T_m)], \qquad i = 1 \text{ or } 2 \tag{6}$$

where q_i is the heat flux from the wall and is positive when fluid is heated by the walls.

Introducing Eq. (1) into Eq. (2) leads to

$$\frac{d^2P(X)}{dX^2} = \frac{-1}{PrU(Y)}\frac{d^4U(Y)}{dY^4} = \text{const, say } \sigma$$

Furthermore, differentiating Eq. (1) with respect to X, one obtains

$$\frac{d^2P}{dX^2} = \sigma = \frac{\partial\theta}{\partial X} \tag{7}$$

Equation (7) implies that the axial temperature gradient is constant in the fully developed region.

In the meanwhile, it is noted that dimensionless mass flow rate may be represented by

$$\int_0^1 U\,dY = Re/Gr \tag{8}$$

We now consider the following thermal boundary conditions of the walls.

Isoflux-Isoflux (Q_1-Q_2)

When the two channel walls are maintained with uniform but not necessarily equal heat fluxes of the first kind combination, the thermal boundary conditions may be expressed by:

At $Y = 0$:

$$U = 0, \qquad (\partial\theta/\partial Y)|_2 = -r_H \tag{9a}$$

At $Y = 1$:

$$U = 0, \qquad (\partial\theta/\partial Y)|_1 = 1 \tag{9b}$$

where $r_H = q_2/q_1$, and $0 \le r_H \le 1$ if wall surface 1 is designated to be hotter.

Integrating Eq. (2) with respect to Y from 0 to 1 and combining Eqs. (7-9), one may show that

$$\sigma Pr = (1 + r_H)/(Re/Gr) \tag{10}$$

If Eq. (1) is differentiated twice with respect to Y and then introduced into Eq. (2), the result becomes

$$\frac{d^4U}{dY^4} + \frac{1 + r_H}{Re/Gr}U = 0 \tag{11}$$

which is a fourth-order O.D.E. subject to boundary conditions

$Y = 0$:

$$U = 0, \qquad \frac{d^3U}{dY^3} = r_H \tag{12a}$$

$Y = 1$:

$$U = 0, \qquad \frac{d^3U}{dY^3} = -1 \tag{12b}$$

where the third-order derivative terms come from Eqs. (1) and (9). Finally, the velocity profile by solving Eqs. (11) and (12) is

$$U(Y) = e^{KY/\sqrt{2}}[C_1\cos(KY/\sqrt{2}) + C_2\sin(KY/\sqrt{2})] + e^{-KY/\sqrt{2}}[C_3\cos(KY/\sqrt{2}) + C_4\sin(KY/\sqrt{2})] \tag{13}$$

where

$$K = [(1 + r_H)/(Re/Gr)]^{1/4}$$

$$C_2 = E_2/E_1, \quad C_3 = E_3/E_1, \quad C_4 = E_4/E_1, \quad C_1 = -C_3$$

and

$$E_1 = -(e^{-K\sqrt{2}} + e^{K\sqrt{2}}) + 4\sin^2(K/\sqrt{2}) + 2$$

$$E_2 = (r_H\sqrt{2}/K^3)[1 + \sin(K\sqrt{2}) - e^{-K\sqrt{2}}] + (2\sqrt{2}/K^3)e^{-K/\sqrt{2}}\sin(K/\sqrt{2}) - (\sqrt{2}/K^3)(e^{-K/\sqrt{2}} - e^{K/\sqrt{2}})\cos(K/\sqrt{2})$$

$$E_3 = (2\sqrt{2}/K^3)r_H\sin^2(K/\sqrt{2}) - (\sqrt{2}/K^3)(e^{-K/\sqrt{2}} - e^{K/\sqrt{2}})\sin(K/\sqrt{2})$$

$$E_4 = (r_H\sqrt{2}/K^3)[1 - \sin(K\sqrt{2}) - e^{K\sqrt{2}}] - (2\sqrt{2}/K^3)e^{K/\sqrt{2}}\sin(K/\sqrt{2}) + (\sqrt{2}/K^3)(e^{-K/\sqrt{2}} - e^{K/\sqrt{2}})\cos(K/\sqrt{2})$$

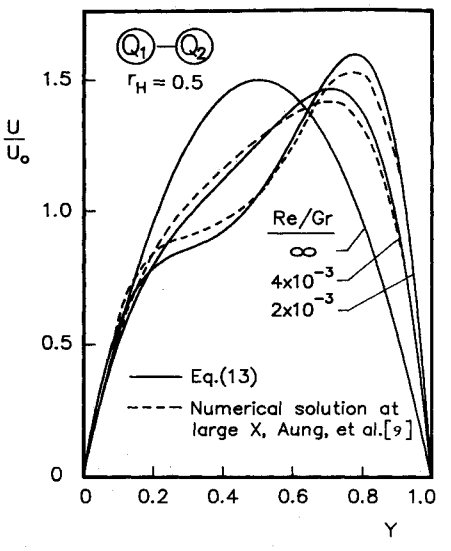

Fig. 2 Comparison of fully developed velocity profiles with developing flow solutions at locations far downstream from Ref. 9, for isoflux-isoflux boundaries.

The velocity solution described by Eq. (13) may be compared for verification with the numerical solution at downstream locations of the developing flow considered by Aung and Worku.[9] Figure 2 shows the results of comparison under various flow rate Re/Gr. The small disagreement between the fully developed flow solution and the asymptotic developing flow solution can be expected since the fully developed result is strictly valid just at very far downstream region of channel.

Figure 3 shows the velocity profiles based on Eq. (13) for $r_H = 1$, 0.5, 0.05, and 0 at smaller values of Re/Gr. For $r_H = 1$ (i.e., symmetric heating), the centerline velocity decreases with Re/Gr, and finally, reversed flow is observed when Re/Gr is lower than 3.2×10^{-4}, as shown in Fig. 3a. This is because at small values of Re/Gr, the stronger buoyant effect accelerates the fluid near the walls so much that the centerline velocity must be retarded to maintain the mass conservation. A similar distortion of velocity profiles can also be found in the asymmetric heating case $r_H = 0.5$ in Fig. 3b. In this case, the critical Re/Gr value for occurrence of reversed flow is 2.5×10^{-4}.

In Figs. 3c and 3d, at a very small r_H the velocity profiles exhibit a marked change in feature as Re/Gr varies. For example, in Fig. 3d, when wall 2 is insulated so that $r_H = 0$, the negative velocity appears adjacent to wall 2 at first. And if the value of Re/Gr keeps going down, the fluid velocity adjacent to wall 2 finally recovers to be positive and the negative-velocity area moves toward the centerline. The variation of velocity profiles can be further illustrated in Fig. 4.

Figure 4 shows the reversed flow zone in an Re/Gr-r_H diagram, which is obtained by performing the numerical calculation of Eq. (13) and indicated with dotted areas. It is noticed that the reversed flow zone is divided into two distinct regions in which the corresponding patterns of reversed-flow velocity profiles are obviously different. However, when the value of r_H is higher than about 0.053, only the double-peak pattern could be seen in the reversed flow zone. The fully developed flow will not have flow reversal outside the dotted areas. This figure clearly confirms the conclusion presented by Aung and Worku[9] that within their studied ranges of parameters, i.e., $0.3 \le r_H \le 1$, $2 \times 10^{-3} \le Re/Gr \le \infty$, no flow reversal was observed.

Let θ_m denote the dimensionless bulk mean temperature with

$$\theta_m = \int_0^1 U\theta\, dY \Big/ \int_0^1 U\, dY = \frac{1}{Re/Gr}\int_0^1 U\theta\, dY \tag{14}$$

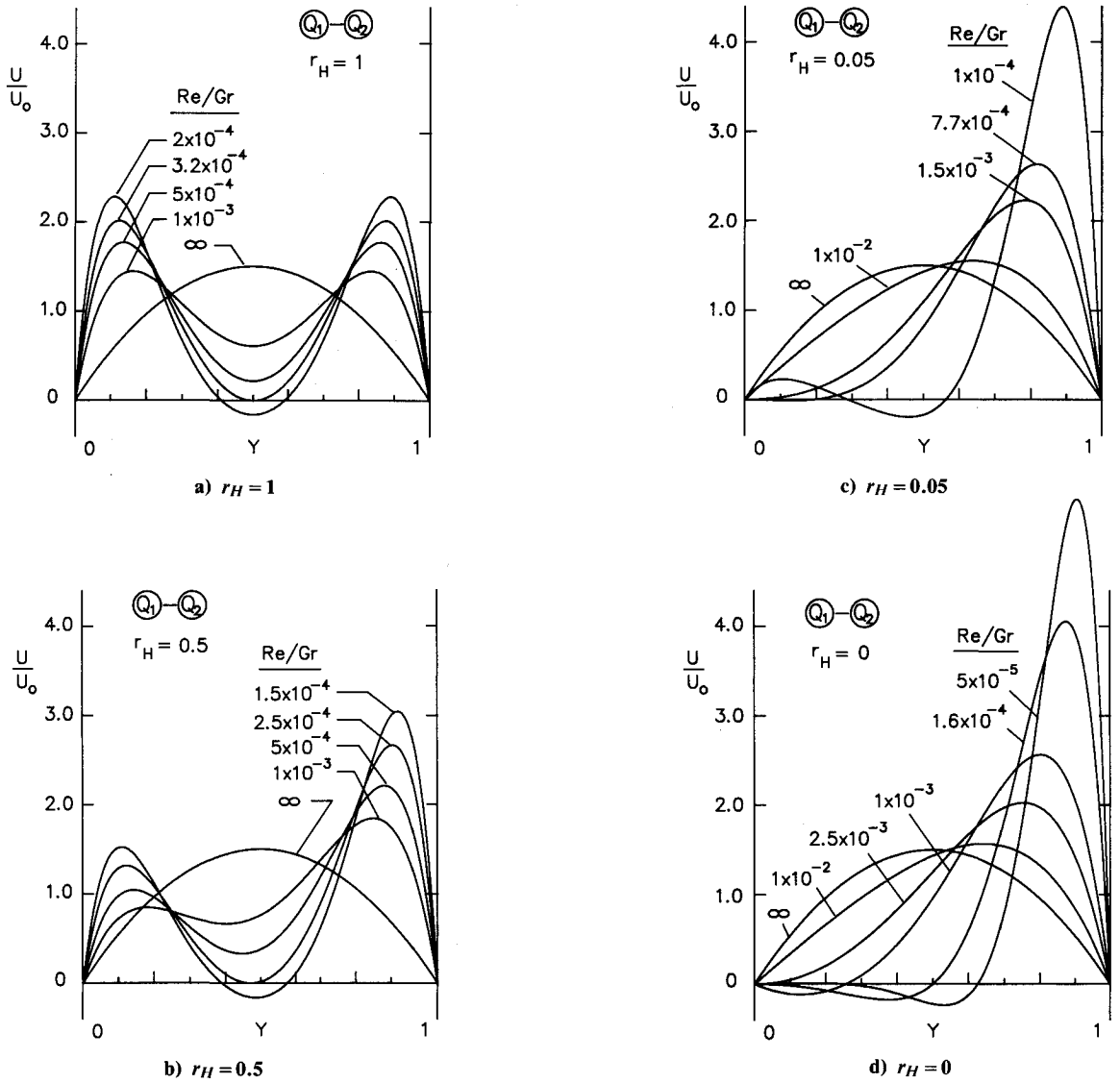

Fig. 3 Velocity profiles under various values of *Re/Gr* for isoflux-isoflux boundaries.

Thus, from the integrations of Eq. (2), one may show that

$$\theta_1 - \theta_m = \frac{1}{Re/Gr}\left[Pr\sigma\int_0^1 U\int_Y^1\int_0^Y U\,dY\,dY\,dY - r_H\int_0^1 U(1-Y)\,dY\right] \tag{15a}$$

and

$$\theta_2 - \theta_m = \frac{1}{Re/Gr}\left(r_H\int_0^1 UY\,dY - Pr\sigma\int_0^1 U\int_0^Y\int_0^Y U\,dY\,dY\,dY\right) \tag{15b}$$

where θ_1 and θ_2 refer to the dimensionless wall temperatures on wall 1 and 2, respectively. According to the definitions of Eq. (6), the Nusselt number on each of the two asymmetrically heated walls can be derived by inserting the known velocity profile, Eq. (13), into the preceding integrals. This leads to

$$Nu_1 = 1/(\theta_1 - \theta_m) = \frac{B^2}{(1+r_H)(BS_1 - A)} \tag{16a}$$

$$Nu_2 = r_H/(\theta_2 - \theta_m) = \frac{-r_H B^2}{(1+r_H)(BS_2 + A)} \tag{16b}$$

where

$$S_1 = (1/K^2)e^{K/\sqrt{2}}[-C_2\cos(K/\sqrt{2}) + C_1\sin(K/\sqrt{2})] + (1/K^2)e^{-K/\sqrt{2}}[C_4\cos(K/\sqrt{2}) - C_3\sin(K/\sqrt{2})]$$

$$S_2 = (C_2 - C_4)/K^2$$

$$A = e^{K\sqrt{2}}[J_1\cos(K\sqrt{2}) + J_2\sin(K\sqrt{2})] + e^{-K\sqrt{2}}[J_3\cos(K\sqrt{2}) + J_4\sin(K\sqrt{2})] - (J_1 + J_3) + H$$

$$B = Re/Gr$$

$$J_1 = (-C_1^2 - 2C_1C_2 + C_2^2)/(4\sqrt{2}K^3)$$

$$J_2 = (C_1^2 - 2C_1C_2 - C_2^2)/(4\sqrt{2}K^3)$$

$$J_3 = (C_3^2 - 2C_3C_4 - C_4^2)/(4\sqrt{2}K^3)$$

$$J_4 = (C_3^2 + 2C_3C_4 - C_4^2)/(4\sqrt{2}K^3)$$

$$H = (C_1C_4 - C_2C_3)/K^2$$

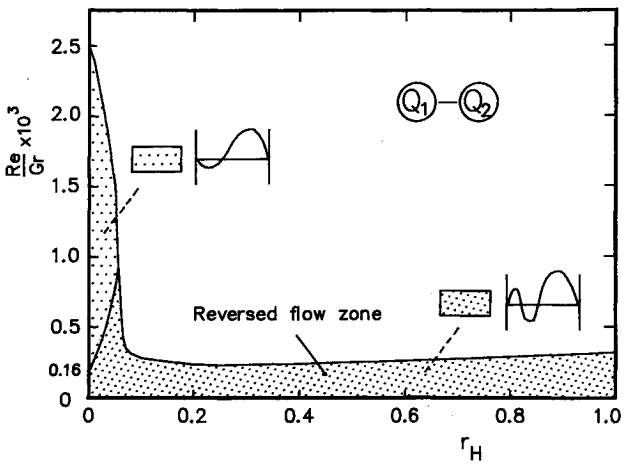

Fig. 4 Reversed flow zone for isoflux-isoflux boundaries.

Table 1 shows some of the numerical results computed from the preceding solutions. It is noted that when Re/Gr is extremely large, the values of Nusselt numbers approach those of pure forced convection because the buoyancy effect could be negligible in this situation.

Isoflux-Isothermal (Q_1)-(T_2)

In this combination, wall 1 is heated with uniform heat flux, and wall 2 is maintained at a constant temperature. The boundary conditions for this case are:

At $Y = 0$:

$$U = 0, \qquad \theta = \theta_2 = 1 \tag{17a}$$

At $Y = 1$:

$$U = 0, \qquad (\partial\theta/\partial Y)|_1 = Q_1 \tag{17b}$$

where $Q_1 = q_1 b/[k(T_2 - T_0)]$, and $Q_1 = 0$ if wall 1 is considered to be insulated.

Since one of the wall surfaces is kept isothermal, the value of σ can be shown to be zero. This indicates that the axial gradient of pressure is a constant value in a fully developed region. Equations (1) and (2) become

$$\frac{d^2U}{dY^2} = \frac{dP}{dX} - \theta \tag{18}$$

$$\frac{d^2\theta}{dY^2} = 0 \tag{19}$$

From Eqs. (17-19), one may obtain the temperature and velocity profiles with

$$\theta = 1 + Q_1 Y \tag{20}$$

$$U(Y) = -Q_1\frac{Y^3}{6} - \frac{Y^2}{2} + (Q_1+3)\frac{Y}{6} + \left(\frac{dP}{dX}\right)\left(\frac{Y^2}{2} - \frac{Y}{2}\right) \tag{21}$$

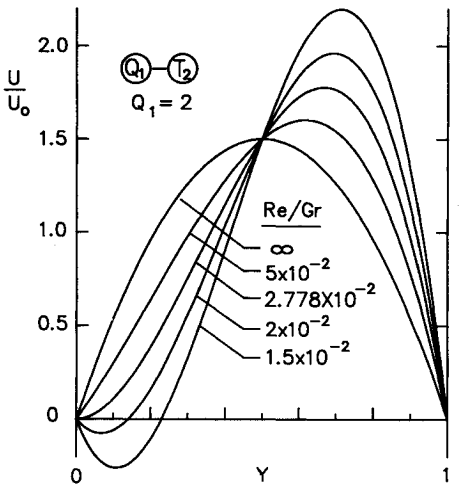

a) Effect of Re/Gr with $Q_1 = 2$

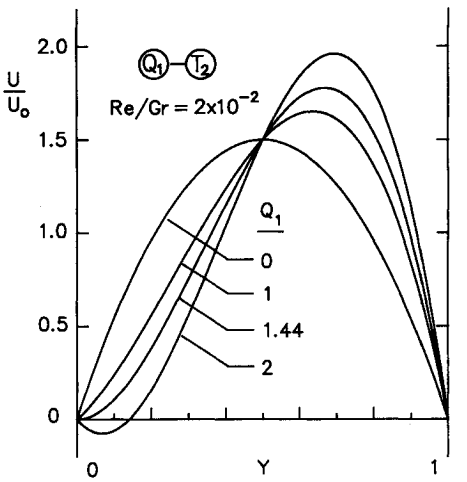

b) Effect of Q_1 with $Re/Gr = 2\times10^{-2}$

Fig. 5 Velocity profiles for isoflux-isothermal boundaries.

where the constant value of dP/dX can be evaluated by performing the integration of velocity profile for mass flow rate. The result is

$$\frac{dP}{dX} = (Q_1 + 2)/2 - 12(Re/Gr) \tag{22}$$

Figure 5 shows the velocity profiles under various values of Re/Gr and Q_1 based on Eq. (21). It is noticed that with low Re/Gr or large Q_1, flow reversal occurs adjacent to the isothermal wall 2. Besides, for this boundary combination, only the single-peak pattern in reversed-flow profiles could be found, not like those of the isoflux-isoflux cases.

Table 1 Nusselt numbers as functions of Re/Gr and r_H for isoflux-isoflux boundaries

(Q_1)-(Q_2)		r_H = 0		0.4		0.5		0.6		1	
		Nu_1	Nu_2	Nu_1	Nu_2	Nu_1	Nu_2	Nu_1	Nu_2	Nu_1	Nu_2
$\frac{Re}{Gr}$	0.001	5.312	0	5.319	9.026	5.403	7.371	5.506	6.695	6.081	6.081
	0.01	3.176	0	3.534	13.984	3.644	7.746	3.764	6.034	4.353	4.353
	0.1	2.745	0	3.172	19.078	3.300	8.611	3.440	6.315	4.141	4.141
	1.0	2.698	0	3.130	19.903	3.260	8.736	3.402	6.359	4.120	4.120
	∞[a]	2.692	0	3.125	20.000	3.256	8.750	3.398	6.364	4.118	4.118

[a]Approach to pure forced convection.

It is helpful to deduce the reversed flow zone in which the flow reversal can be predicted to occur. For the polynomial expression of velocity in Eq. (21), the occurrence of flow reversal is ensured if

$$\left[\frac{dU}{dY}\bigg|_{Y=0}\right]\cdot\left[\frac{dU}{dY}\bigg|_{Y=1}\right]\geq 0 \tag{23}$$

In the meantime, considering the buoyancy-assisted flow with positive mass flow rate, one may deduce the reversed flow zone in terms of pressure gradient as

$$\frac{(Q_1+3)}{3}\leq\frac{dP}{dX}\leq\frac{(Q_1+2)}{2} \tag{24}$$

Or by using Eq. (22), the reversed flow zone can alternatively be expressed in terms of Re/Gr. That is

$$0\leq Re/Gr\leq Q_1/72 \tag{25}$$

Figure 6 shows the reversed flow zones, given by Eqs. (24) and (25) in $dP/dX-Q_1$ and $Re/Gr-Q_1$ diagrams, respectively. It is noticed that when $Q_1=0$, there is no flow reversal in fully developed flow. Nevertheless, a larger Q_1 gives rise to the stronger buoyant effect and, hence, makes flow reversal easier to occur near the relatively colder wall 2. In Fig. 6a, the buoyancy-assisted flow region is emphatically indicated with an arrow mark. The upper portion of this figure [i.e., $dP/dX\geq(Q_1+2)/2$] refers to the buoyancy-resisted flow, which is not considered in this study.

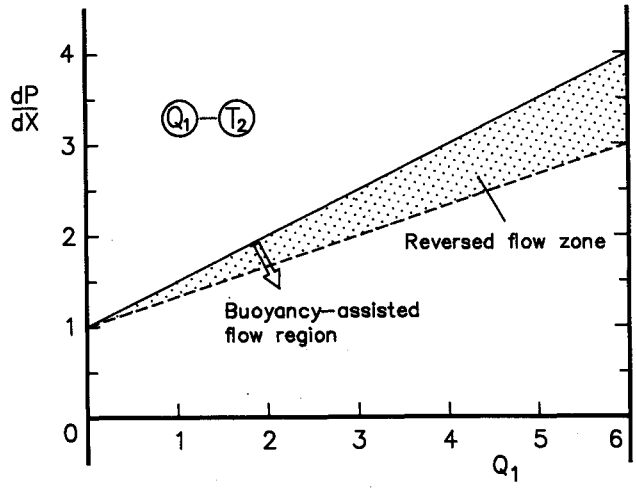

a) dP/dX-Q_1 diagram

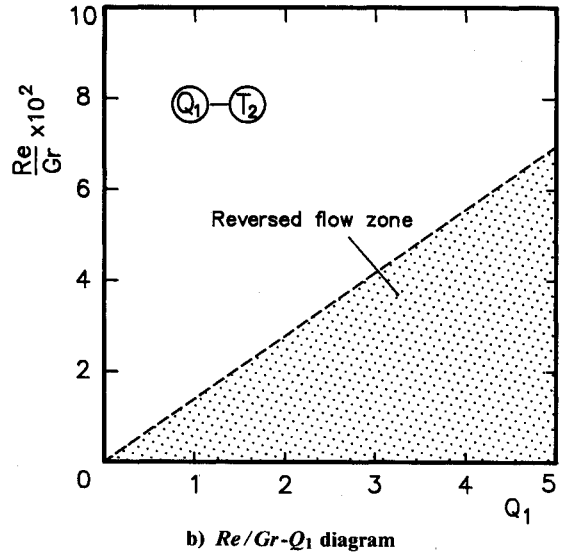

b) Re/Gr-Q_1 diagram

Fig. 6 Reversed flow zone for isoflux-isothermal boundaries.

Through a further examination of Eq. (21), one may show that the negative-velocity extent appears only within

$$0\leq Y\leq 1/2$$

Thus, it means that the flow reversal can only be found in the left half of the channel space.

According to Eqs. (14), (20), and (21), the bulk mean temperature is

$$\theta_m=(Q_1+2)/2+Q_1^2/[720(Re/Gr)] \tag{26}$$

which leads to the Nusselt numbers

$$Nu_1=-\frac{\partial}{\partial Y}\left(\frac{\theta_1-\theta}{\theta_1-\theta_m}\right)\bigg|_{Y=1}=\frac{720(Re/Gr)}{360(Re/Gr)-Q_1} \tag{27a}$$

$$Nu_2=\frac{\partial}{\partial Y}\left(\frac{\theta_2-\theta}{\theta_2-\theta_m}\right)\bigg|_{Y=0}=\frac{720(Re/Gr)}{360(Re/Gr)+Q_1} \tag{27b}$$

where θ_1 and θ_2 represent the wall temperatures for walls 1 and 2, respectively.

It is important to note that Eqs. (27) are valid for the cases of $Q_1\neq 0$ but cannot be applied to those of $Q_1=0$. For $Q_1=0$, Eq. (20) reduces to $\theta=\theta_1=\theta_2=\theta_m=1$. Thus, Eqs. (27) may not be used directly to yield Nusselt numbers in this situation.

The Nusselt number on wall 1, Nu_1, becomes 0 if $Q_1=0$; meanwhile, the first derivative term of θ in Eq. (2) can be replaced with $\bar{\theta}_2(d\theta_m/dX)$, where $\bar{\theta}_2=(\theta_2-\theta)/(\theta_2-\theta_m)$, even though σ is proved to be zero. The newly obtained equation is then integrated twice with respect to Y to yield

$$\theta_2-\theta=Pr\left(\frac{d\theta_m}{dX}\right)\int_0^Y\int_Y^1 U\bar{\theta}_2\,dY\,dY$$

and

$$\theta_2-\theta_m=\frac{1}{Re/Gr}Pr\left(\frac{d\theta_m}{dX}\right)\int_0^1 U\int_0^Y\int_Y^1 U\bar{\theta}_2\,dY\,dY\,dY$$

Thus, one can have

$$\bar{\theta}_2=\frac{\dfrac{Re}{Gr}\displaystyle\int_0^Y\int_Y^1 U\bar{\theta}_2\,dY\,dY}{\displaystyle\int_0^1 U\int_0^Y\int_Y^1 U\bar{\theta}_2\,dY\,dY\,dY} \tag{28a}$$

$$Nu_2=\frac{\dfrac{Re}{Gr}\displaystyle\int_0^1 U\bar{\theta}_2\,dY}{\displaystyle\int_0^1 U\int_0^Y\int_Y^1 U\bar{\theta}_2\,dY\,dY\,dY} \tag{28b}$$

The velocity $U(Y)$ being known, Nu_2 can be determined by solving Eqs. (28) through the successive approximation. A polynomial profile of $\bar{\theta}_2$ satisfying the boundary conditions is initially assumed and substituted into the right side of Eq. (28a). Performing the integrations yields an improved profile. The process is repeated until the value of the Nusselt number, evaluated from Eq. (28b) in each iteration, converges. Only several iterations are sufficient for the convergence with absolute relative error of 10^{-5}, and one can find

$$Nu_2=2.43047 \tag{29}$$

which is identical to the value of the well-known pure forced convection flow and is independent of Re/Gr even though

Table 2 Nusselt numbers as functions of Re/Gr and Q_1 for isoflux-isothermal boundaries

(Q_1)-(T_2)		Q_1 = 0		Q_1 = 1		Q_1 = 2		Q_1 = 3	
		Nu_1	Nu_2	Nu_1	Nu_2	Nu_1	Nu_2	Nu_1	Nu_2
	0.01	0	2.430	2.769	1.565	4.500	1.286	12.00	1.091
Re	0.1	0	2.430	2.057	1.946	2.118	1.895	2.182	1.846
Gr	1.0	0	2.430	2.006	1.994	2.011	1.989	2.017	1.983
	∞[a]	0	2.430	2.000	2.000	2.000	2.000	2.000	2.000

[a]Approach to pure forced convection.

Re/Gr explicitly appears in Eqs. (28). This result confirms the numerical solutions of Habchi and Acharya[10] at far downstream locations of the developing flow under such an asymmetric heating condition.

Table 2 shows the Nusselt numbers as functions of Re/Gr and Q_1, based on Eqs. (27) and (29). Similarly, it is found that if Re/Gr goes to infinity, Nusselt numbers approach to those of pure forced convection flow.

Isothermal-Isothermal $((T_1)$-$(T_2))$

In this case, the walls are maintained with uniform but not necessarily equal wall temperatures. The expressions are

At $Y = 0$:

$$U = 0, \qquad \theta = \theta_2 = r_T \tag{30a}$$

At $Y = 1$:

$$U = 0, \qquad \theta = \theta_1 = 1 \tag{30b}$$

where $r_T = (T_2 - T_0)/(T_1 - T_0)$ with T_1 and T_2 referring to the wall temperatures of wall 1 and 2, respectively. One may have $0 \le r_T \le 1$ if wall surface 1 is considered to be the hotter surface.

By solving Eqs. (18), (19), and (30), the solutions of velocity profile, temperature profile, and bulk mean temperature for this boundary combination had been carried out by Aung and Worku,[11] and the reversed flow zone was also discussed. Hence, additional derivation about their solutions may not be necessary. Figure 7 shows the reversed flow pattern from their solutions under various values of Re/Gr and r_T. It is obvious that only the single-peak pattern in reversed flow profile could be found, and the negative-velocity area is immediately adjacent to the colder wall.

However, based on the solutions, it can be deduced that the flow reversal occurs in the buoyancy-assisted flow if

$$(2r_T + 1)/3 \le \frac{dP}{dX} \le (r_T + 1)/2 \tag{31}$$

or, alternatively, if

$$0 \le \frac{Re}{Gr} \le (1 - r_T)/72 \tag{32}$$

Figure 8 shows the reversed flow zones defined by Eqs. (31) and (32), respectively. It is clearly noticed that the flow reversal occurs most possibly when $r_T = 0$. Only the single-peak pattern in reversed flow profile could be found, and the negative-velocity area is immediately adjacent to the colder wall.

By following a procedure rather similar to the procedure in the isoflux-isothermal combination, the Nusselt numbers on the respective isothermal walls with $T_1 \neq T_2$ can be obtained with

$$Nu_1 = \frac{720(Re/Gr)}{360(Re/Gr) + r_T - 1} \tag{33a}$$

$$Nu_2 = \frac{720(Re/Gr)}{360(Re/Gr) - r_T + 1} \tag{33b}$$

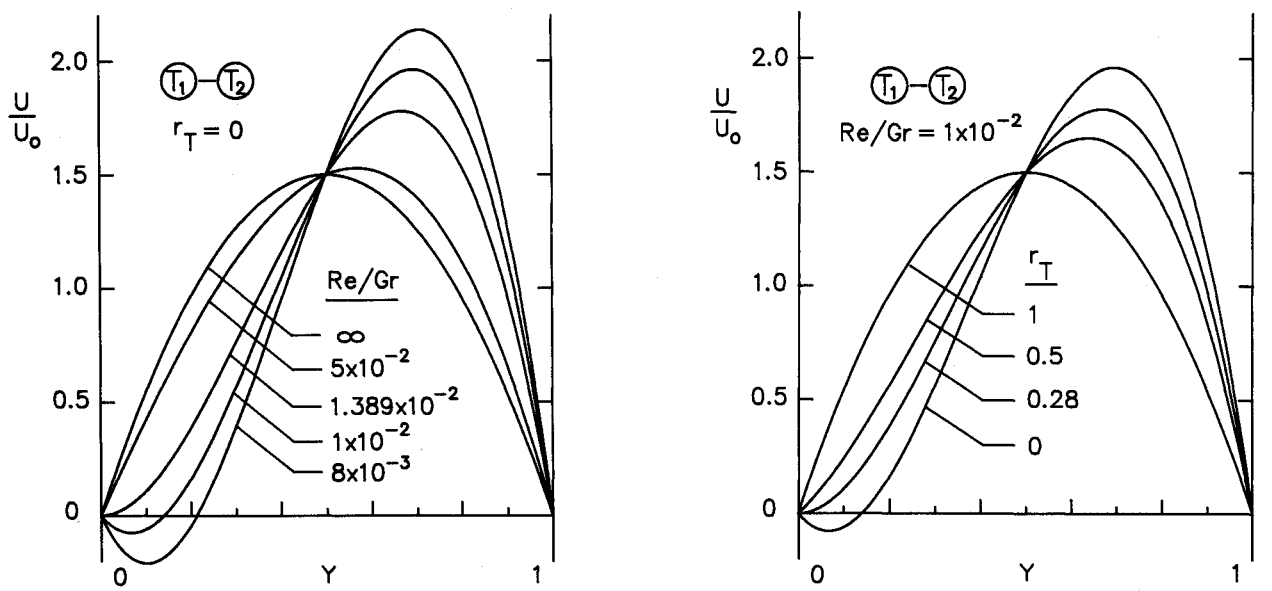

a) Effect of Re/Gr with $r_T = 0$

b) Effect of r_T with $Re/Gr = 1 \times 10^{-2}$

Fig. 7 Velocity profiles for isoflux-isoflux boundaries.

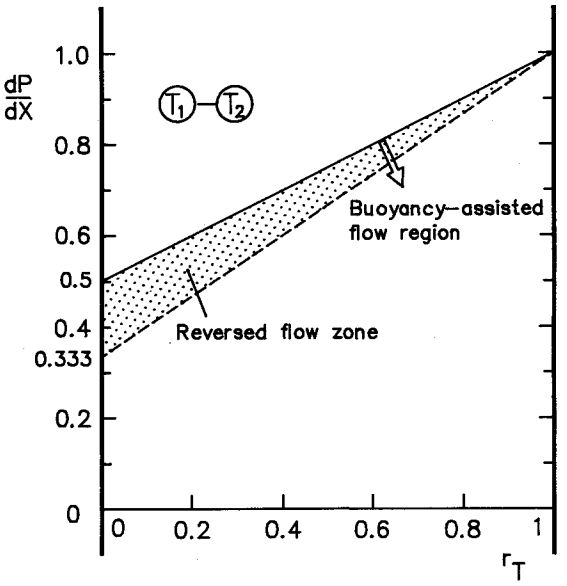

a) dP/dX-r_T diagram

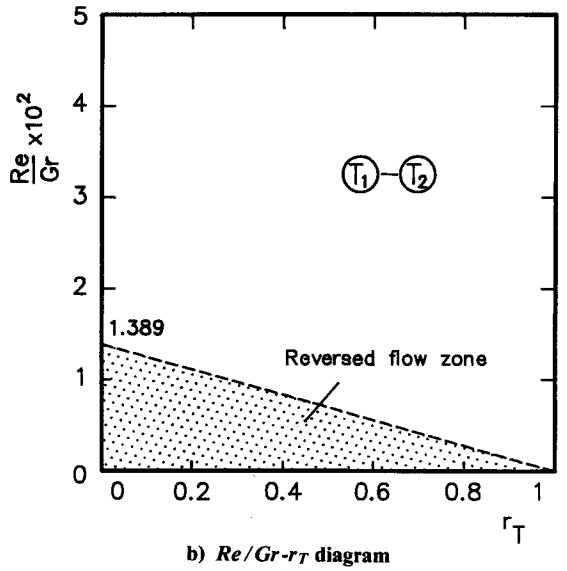

b) Re/Gr-r_T diagram

Fig. 8 Reversed flow zone for isothermal-isothermal boundaries.

In the meanwhile, for the cases of $T_1 = T_2$ (i.e., symmetric heating), the results are

$$\bar{\theta}_1 = \frac{\left(\frac{Re}{Gr}\right)\left[Y\int_0^1\int_0^Y U\bar{\theta}_1\,dY\,dY - \int_0^Y\int_0^Y U\bar{\theta}_1\,dY\,dY\right]}{\int_0^1 UY\int_0^1\int_0^Y U\bar{\theta}_1\,dY\,dY\,dY - \int_0^1 U\int_0^Y\int_0^Y U\bar{\theta}_1\,dY\,dY\,dY} \tag{34a}$$

$$Nu_1 = Nu_2 = \frac{\left(\frac{Re}{Gr}\right)\int_0^1\int_0^Y U\bar{\theta}_1\,dY\,dY}{\int_0^1 UY\int_0^1\int_0^Y U\bar{\theta}_1\,dY\,dY\,dY - \int_0^1 U\int_0^Y\int_0^Y U\bar{\theta}_1\,dY\,dY\,dY} \tag{34b}$$

By means of the successive approximation just described, one obtains

$$Nu_1 = Nu_2 = 3.77052 \tag{35}$$

Table 3 Nusselt numbers as functions of Re/Gr and r_T for isothermal-isothermal boundaries

		r_T = 0		0.5		1	
(T1)-(T2)		Nu_1	Nu_2	Nu_1	Nu_2	Nu_1	Nu_2
	0.01	2.769	1.565	2.323	1.756	3.770	3.770
Re	0.1	2.057	1.946	2.028	1.973	3.770	3.770
Gr	1.0	2.006	1.994	2.003	1.997	3.770	3.770
	∞[a]	2.000	2.000	2.000	2.000	3.770	3.770

[a]Approach to pure forced convection.

which is not influenced by the variation of Re/Gr. This theoretical value confirms the numerical asymptotic solutions of Habchi et al.[10] for the developing flow under symmetric isothermal heating. Some numerical results from Eqs. (33) and (35) are provided in Table 3.

Conclusions

The laminar fully developed characteristics, especially the flow reversal phenomena and the Nusselt numbers, of the combined free and forced convection in the vertical parallel plate channels are investigated theoretically. Three different thermal boundary conditions on the respective wall surfaces are considered separately in this study. They are isoflux-isoflux, isoflux-isothermal, and isothermal-isothermal, which cover all the symmetric or asymmetric thermal boundary conditions considered by the previous investigators. Thus, the present analysis complements and unifies the related existing solutions.

The occurrence of reversed flow is found to be strongly dependent on the value of Re/Gr and the thermal boundary condition. Reversed flow zone in parameters (or say, the criterion of flow reversal occurrence) for each thermal boundary combination has been carried out theoretically, according to the obtained solution of velocity. It is noted that there are two possible patterns of reversed-flow velocity profile for the isoflux-isoflux boundary, whereas only the single-peak pattern with a negative-velocity area adjacent to the colder wall could be found for the isoflux-isothermal or isothermal-isothermal boundary.

On the other hand, the Nusselt numbers in terms of bulk mean temperature are constant in the fully developed region. Closed-form expressions of Nusselt numbers on the respective walls are presented for each thermal boundary condition. Results show that for $Q_1 = 0$ in isoflux-isothermal cases and $T_1 = T_2$ in isothermal-isothermal cases, Nusselt numbers are found identical with the values of pure forced convection flow and independent of Re/Gr. But for other thermal boundary conditions considered herein, the values are a function of Re/Gr and are affected by the heating conditions on the walls.

The fully developed solutions presented in this study portray the behavior of developing flows at far downstream locations. Some comparisons have hence been made for verification by using the existing numerical solutions of the developing flows.[8-10]

References

[1]Hanratty, T. J., Rosen, E. M., and Kabel, R. L., "Effect of Heat Transfer on Flow Field at Low Reynolds Numbers in Vertical Tubes," *Industrial Engineering Chemistry*, Vol. 50, 1958, pp. 815–820.

[2]Kim, J. H., "Analysis of Laminar Mixed Convection in Vertical Tube Annulus with Upward Flow," *Fundamentals of Forced and Mixed Convection*, edited by F. A. Kulacki and R. D. Boyd, ASME, New York, HTD-Vol. 42, 1985, pp. 91–98.

[3]Maitra, D., and Raju, K. S., "Combined Free and Forced Convection Laminar Heat Transfer in a Vertical Annulus," *Journal of Heat Transfer*, Feb. 1975, pp. 135–137.

[4]Aggarwala, B. D., and Iqbal, M., "On Limiting Nusselt Numbers from Membrane Analogy for Combined Free and Forced Convection through Vertical Ducts," *International Journal of Heat and Mass Transfer*, Vol. 12, 1969, pp. 737–748.

[5]Iqbal, M., and Aggarwala, B. D., "Combined Free and Forced Convection through Vertical Rectangular Channels with Unequal Heating from Sides," *Journal of Applied Mechanics,* Dec. 1971, pp. 829-833.

[6]Iqbal, M., Aggarwala, B. D., and Fowler, A. G., "Laminar Combined Free and Forced Convection in Vertical Non-Circular Ducts under Uniform Heat Flux," *International Journal of Heat and Mass Transfer,* Vol. 12, 1969, pp. 1123-1139.

[7]Efthimiadis, A., and Todreas, N. E., "Generalized Formulation of the Fully-Developed Mixed Convection Flow Problem in Vertical Ducts," *Fundamentals of Forced and Mixed Convection,* edited by F. A. Kulacki and R. D. Boyd, ASME, New York, HTD-Vol. 42, 1985, pp. 83-89.

[8]Aung, W., and Worku, G., "Developing Flow and Flow Reversal in a Vertical Channel with Asymmetric Wall Temperatures," *Journal of Heat Transfer,* Vol. 108, 1986, pp. 299-304.

[9]Aung, W., and Worku, G., "Mixed Convection in Ducts with Asymmetric Wall Heat Fluxes," *Journal of Heat Transfer,* Vol. 109, 1987, pp. 947-951.

[10]Habchi, S., and Acharya, S., "Laminar Mixed Convection in a Symmetrically or Asymmetrically Heated Vertical Channel," *Numerical Heat Transfer,* Vol. 9, 1986, pp. 605-618.

[11]Aung, W., and Worku, G., "Theory of Fully Developed, Combined Convection Including Flow Reversal," *Journal of Heat Transfer,* Vol. 108, 1986, pp. 485-488.